Electron spin–orbit split minibands in semiconductor asymmetric superlattices

C. Moysés Araújo and Antonio Ferreira da Silva
Instituto de Física, Universidade Federal da Bahia 40210-340, Salvador, Bahia, Brazil

Erasmo A. de Andrada e Silva
Instituto Nacional de Pesquisas Espaciais - INPE, C.P. 515, 12201-900, São José dos Campos, São Paulo, Brazil
(Received 6 December 2001; published 24 May 2002)

Semiconductor superlattices can be either symmetric or asymmetric with respect to specular reflection along the growth direction. The electronic miniband structure of asymmetric superlattices is in general spin dependent, due to spin–orbit interaction. Using Kane's $\mathbf{k}\cdot\mathbf{p}$ model for the bulk and standard envelope function formalism, we have calculated the spin dependent transmission probability for electrons crossing different III–V politype multibarrier nanostructures. We have obtained spin dependent intervals of energy with nonzero transmission, corresponding to the minibands of allowed electronic states in the superlattice. Spin–orbit split minibands for InGaAs superlattices, with asymmetric double barrier unit cells and different pairs of lattice-matched barrier materials, are obtained from the transmission and reflection coefficients for the unit cell. The miniband structure is well reproduced by the transfer matrix calculation with already three unit cells. The symmetric–asymmetric crossover as well as the miniband formation from the double barrier spin split resonances were also investigated. The effect of electron spin polarization by resonant tunneling is shown to be enhanced with the use of multibarrier or superlattice structures.

DOI: 10.1103/PhysRevB.65.235305 PACS number(s): 73.21.−b, 71.70.Ej, 73.20.−r

I. INTRODUCTION

The physics of the transport of spin polarized electrons in semiconductor nanostructures is fundamental in the new generation of semiconductor devices that form what has been called spintronics or spin electronics.[1] In order to perform new functions and better perform the usual ones, such devices intend to take advantage of the electron spin degree of freedom, which has not been playing a role in the standard microelectronic technology. There is today an increasing research effort to develop the physics of the spin dependent electronic properties of semiconductor and semiconductor–metal hybrid nanostructures. It is still not clear for example how to inject,[2] detect, and transport[3] polarized electrons with enough control in these nanostructures. The spin–orbit coupling, together with the advanced semiconductor orbital engineering, represents an important tool in this effort to control the electron spin degree of freedom in semiconductor nanostructures.

In fact, the functioning of the spin transistor, the main proposal of a spintronic device so far,[4] is based on the control over the spin polarization of the conducting electrons confined in a heterojunction, with the gate voltage, through the so called Rashba spin-orbit coupling.[5] Such spin dependent term in the Hamiltonian describing the motion of electrons in semiconductor nanostructures, breaks the spin degeneracy of the electronic states allowed in asymmetric structures, as formed, for example, at the interface of semiconductor heterojunctions.[6] The corresponding spin splitting between the states with opposite spins is, in first order, linear with the electron in-plane (or parallel) wave vector $k_{\parallel}$, and can be described as the action of an effective magnetic field which is perpendicular to both the growth and $k_{\parallel}$ directions.[7] Besides the spin precession effect, around the effective field during in-plane motion, in which the spin transistor is based, the Rashba spin–orbit coupling can lead also to spin dependent vertical transport or resonant tunneling effects.

It has been shown that the spin dependent resonant tunneling of electrons, in asymmetric double barrier nonmagnetic semiconductor structures, can be used as the basic principle of a possible new kind of electron beam polarizer.[8,9] The electron transmission through asymmetric structures, in the presence of Rashba spin–orbit interaction, is spin dependent whenever the incidence is not normal, corresponding to electron tunneling with nonzero and conserved $k_{\parallel}$. The transmission then presents spin dependent resonances corresponding to tunneling at energies in resonance with the spin split quasibound electronic states of the double barrier structure. The effect optimization, with respect to the choice of materials and structure parameters to be used in specific applications, has however, not been done yet. In particular, it would be interesting to consider more general multibarrier structures as well as the miniband transport of polarized electrons in asymmetric semiconductor superlattices.

In this work we present a study of the quantum coherent or resonant tunneling spin dependent transport of electrons along multibarrier and superlattice nonmagnetic III–V semiconductor nanostructures, with asymmetric double barrier unit cells. Using standard envelope function approximation for the nanostructure calculation, with Kane's $\mathbf{k}\cdot\mathbf{p}$ model to describe the bulk, we have calculated the spin dependent transmission probability, as a function of electron energy, and the superlattice miniband structure for specific InGaAs multibarrier and superlattice structures, with lattice-matched GaAsSb, InP, and InAlAs barriers. Well defined spin–orbit split minibands are obtained which, in the ideal case, lead to perfect modulated spin filtering. Next, we first say a few words on the multibarrier and superlattice specular symmetry. Then, in Sec. III, we present the multibarrier calculation of the polarized electron transmission probability; and, in

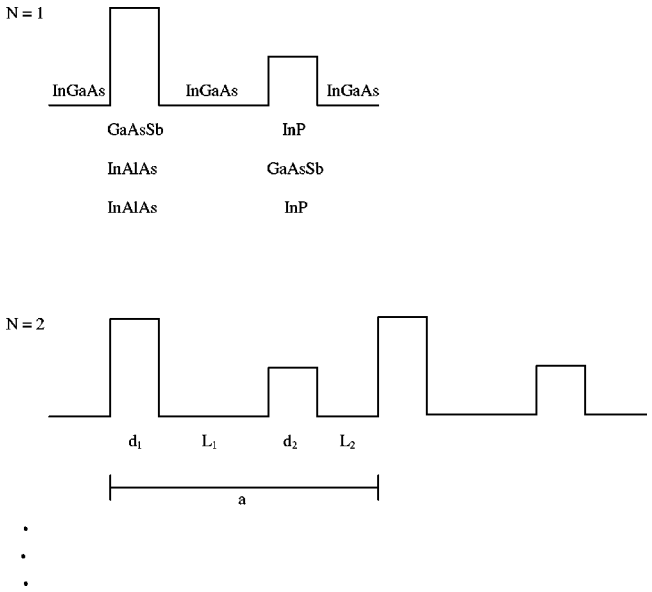

FIG. 1. Illustration of the conduction band profile of the multibarrier and superlattice structures studied, with its parameters. *N* gives the number asymmetric double-barrier unit cells. It is also signed the different combinations of lattice-matched barrier materials in an InGaAs matrix.

Sec. IV, we discuss the solution for the asymmetric superlattice problem and the formation of the spin–orbit split minibands. The main results are summarized in the Conclusions.

II. MULTIBARRIER AND SUPERLATTICE SPECULAR SYMMETRY

Superlattices are important realizations of ideal one-dimensional solids. They are characterized by their unit cell and can be classified in accord to its specular symmetry along the growth direction. An asymmetric unit cell is necessary but not sufficient to construct a superlattice without mirror symmetry. In this work, we consider asymmetric double barrier unit cell multibarrier and superlattice structures, with the conduction band profile, as well as the parameters, illustrated in Fig. 1. Note that if L_1 or L_2 is zero, we have simple asymmetric single barrier cells and that unit cells with three or more barriers do not introduce qualitative new physics, so that the class of superlattices considered here is quite general. The asymmetry of the superlattices with such double-barrier cells, with different barrier materials 1 and 2, is independent of d_1 and d_2, the respective barrier widths, and, for simplicity, we will then use only thin barriers with the same width $d_1=d_2=3$ nm.[12] The asymmetry in this case depends only on the width of the InGaAs layers.

The superlattice structures illustrated in Fig. 1 can be symmetric or asymmetric depending on whether L_1 and L_2 are equal or different. The corresponding finite multibarrier systems are allways asymmetric, except with $L_1=L_2$ when its degree of asymmetry decreases with increasing number N of unit cells, tending to the superlattice ($N=\infty$) limit, which is symmetric under reflections at the center of any barrier. In any case, the structures that interest us most here, for the spin dependent properties, are the asymmetric ones. The results, discussed in the next section, for the calculation of the spin dependent electron transmission probability through multibarrier structures are well explained by this symmetry.

TABLE I. Bulk parameters used in the calculations; band gap, spin–orbit splitting Δ, electron effective mass (Ref. 10), and conduction band offsets (Ref. 11) for $In_{0.53}Ga_{0.47}As$ lattice-matched III–V semiconductor.

	E_g(eV)	Δ(eV)	$m_e^*(m_e)$	V(meV)
$In_{0.53}Ga_{0.47}As$	0.75	0.36	0.041	0
InP	1.42	0.11	0.079	180
$GaAs_{0.5}Sb_{0.5}$	0.81	0.75	0.040	360
$In_{0.52}Al_{0.48}As$	1.47	0.33	0.078	520

III. MULTIBARRIER TRANSFER MATRIX CALCULATION

It is common to use multiple quantum wells and barriers to enhance single well and barrier effects in semiconductor nanostructures.[13] In this paper, we apply the same idea for the spin polarization by the resonant tunneling effect.[8] Besides, in the present superlattice problem, the multibarrier structures, with a finite number N of unit cells, is of interest for at least two main reasons: in view of the fact that real superlattice samples are finite and because it can clarify the way the superlattice spin dependent miniband structure develops from the single asymmetric double barrier case studied in Refs. 8,9

The calculation, which follows closely the transfer method presented in Ref. 8, consider the III–V semiconductor multibarrier structures illustrated in Fig. 1, which uses $In_{0.53}Ga_{0.47}As$ III–V compound as host material and three different lattice matched barriers (InP, $In_{0.48}Al_{0.52}As$, and $GaAs_{0.5}Sb_{0.5}$), that allow the growth of different asymmetric multibarrier and superlattice structures with varying spin–orbit coupling. Starting from Kane's **kp** model, the transmission probability for electrons in the conduction band, with spin up or down along the effective magnetic field, in the zero bias or flat band approximation, can be easily calculated using simple plane wave solutions satisfying the spin dependent boundary conditions for the envelope function.[14] It is obtained as a function of both electron energy E and $k_\parallel = \sqrt{2m_0E/\hbar^2}\sin(\theta)$, where θ is the angle of incidence and $m_0=m_0(E)$ is the energy dependent effective mass of the electron in the InGaAs layers. For III–V semiconductor compounds described by Kane's model, the expression for such effective mass reads

$$\frac{1}{m_i(E)}=\frac{P^2}{\hbar^2}\left(\frac{2}{E-E_{c,i}+E_{g,i}}+\frac{1}{E-E_{c,i}+E_{g,i}+\Delta_i}\right), \qquad (1)$$

where E_g, the band gap, and Δ, the spin–orbit splitting in the top of the bulk valence band, are band parameters listed in Table I. The interband momentum matrix element P is determined by the band edge effective mass listed in the third column and E_c stands for the conduction band edge (note

that if we set $E_{c,0}=0$, $E_{c,i}$ will then be equal to the conduction band offset, or barrier height, listed in the last column of Table I).

Both transmission and reflection spin dependent coefficients, $t_\pm$ and $r_\pm$ (with $\pm$ corresponding to spin up and down, respectively), for a multibarrier structure with N double-barrier unit cells, will then be obtained by solving the following equations:

$$\begin{pmatrix} t_\pm \\ 0 \end{pmatrix} = M_\pm^N \begin{pmatrix} e^{ik_z Na} & 0 \\ 0 & e^{-ik_z Na} \end{pmatrix} \begin{pmatrix} 1 \\ r_\pm \end{pmatrix}, \tag{2}$$

with

$$M_\pm = B_\pm^{(1)} \begin{pmatrix} e^{-ik_z w_1} & 0 \\ 0 & e^{ik_z w_1} \end{pmatrix} B_\pm^{(2)} \begin{pmatrix} e^{-ik_z w_2} & 0 \\ 0 & e^{ik_z w_2} \end{pmatrix}, \tag{3}$$

where $w_i=d_i+L_i$, $a(=w_1+w_2)$ is the multibarrier or superlattice period and $B_\pm^{(j)}$ is the spin dependent transfer matrix for tunneling across the jth-barrier, obtained in Ref. 8 and which is given by

$$B_\pm^{(j)} = \frac{m_0 m_j}{2k_z \rho_j} \sinh(\rho_j d_j) \begin{pmatrix} e^{-ik_z d_j} & 0 \\ 0 & e^{ik_z d_j} \end{pmatrix} \begin{pmatrix} P & Q_\pm \\ Q_\pm^* & P^* \end{pmatrix} \tag{4}$$

with

$$P = \frac{2k_z \rho_j}{m_0 m_j} \frac{1}{\tanh(\rho_j d_j)} + i\left[\left(\frac{2k_\parallel}{\hbar^2} \right)^2 (\beta_0 - \beta_j)^2 + \left(\frac{k_z^2}{m_0^2} - \frac{\rho_j^2}{m_j^2} \right) \right], \tag{5}$$

and

$$Q_\pm = \pm \frac{4k_z k_\parallel}{\hbar^2 m_0} (\beta_0 - \beta_j) + i\left[\left(\frac{2k_\parallel}{\hbar^2} \right)^2 (\beta_0 - \beta_j)^2 - \left(\frac{k_z^2}{m_0^2} + \frac{\rho_j^2}{m_j^2} \right) \right]. \tag{6}$$

The wave vector along the growth direction k_z is given by $\sqrt{2m_0(E-E_{c0})/\hbar^2}\cos(\theta)$, and the decay coefficient of the evanescent wave inside the jth-barrier is $\rho_j = \sqrt{(2m_j/\hbar^2)(E_{cj}-E)+k_\parallel^2}$ [we are interested in resonant tunneling effects and work with $E \leqslant \min(E_{c1},E_{c2})$]. Finally, the spin–orbit coupling parameter β_j as given by Kane's model is given by

$$\beta_j = \frac{P^2}{2}\left(\frac{1}{E-E_{cj}+E_{g,j}} - \frac{1}{E-E_{cj}+E_{g,j}+\Delta_j} \right). \tag{7}$$

In Fig. 2 we show the results for the transmission probability obtained for electrons with both spins traversing multibarrier structures with three and five double barrier unit cells (i.e., with six and ten barriers), $L_1=L_2=20$ nm and compare with those obtained for the single double barrier, shown on top. The angle of incidence is set $\theta=\pi/4$. One can see that the spin split resonances of the double barrier develop into two spin degenerate energy minibands with nonzero transmission, in accord with the expected spin degenerate minibands of the corresponding infinite symmetric superlattice. The behavior in the case of multibarrier structures leading to asymmetric superlattices is very different.

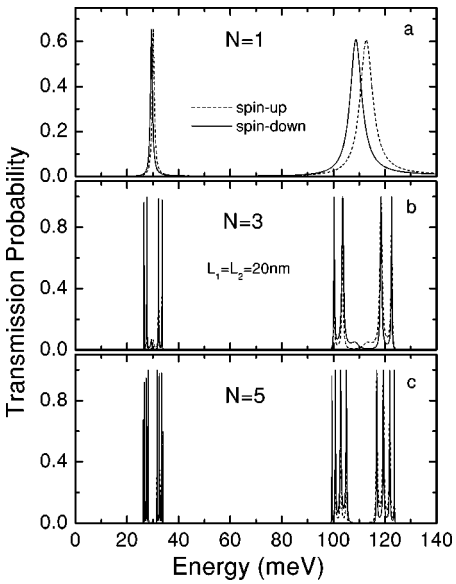

FIG. 2. Spin dependent transmission probability for electrons tunneling, with an angle $\theta=\pi/4$ with respect to the growth direction, across one (a), three (b), and five (c) asymmetric double-barrier unit cells of lattice-matched $In_{0.53}Ga_{0.47}As/InP/In_{0.53}Ga_{0.47}As/GaAs_{0.5}Sb_{0.5}/In_{0.53}Ga_{0.47}As$, with $L_1=L_2=20$ nm and $d_1=d_2=3$ nm—the symmetric case. The band parameters and offsets used are listed in Table I.

An example of asymmetric ($L_1 \neq L_2$) structure is considered in Fig. 3, where we show the results for the same structures of Fig. 2 except for the smaller $L_2=15$ nm. The evolution, as we add more cells, is now different. The opposite spin resonances now develop into two sets of spin-split minibands, with one pushed to higher energies, corresponding to the states bound to the narrower well. With increasing N, we obtain the superlattice spin–orbit split minibands shown in the panel (d) and discussed in detail in the next section. It is interesting to have another look at this symmetric-asymmetric crossover. In Fig. 4 one can see that, as we move from the $L_1=L_2=20$ nm symmetric case, by reducing L_2, the almost spin degenerate minibands start soon to split into opposite spin minibands. The higher energy minibands, in each pair, corresponding to resonance transmission through the states quasibound to the narrow wells, are pushed up in energy due to the bigger quantum confinement. It is worth to mention that reducing L_2 the specular asymmetry increases, enlarging the spin–orbit splitting.

The dependence of the transmission probability on $k_\parallel$ (or angle of incidence), not shown, is very simple. With increasing $k_\parallel$ the resonances or minibands are simply pushed to higher energies, where the spin splittings are bigger, as first observed and explained in Ref. 8. Figure 3 shows that the minibands of perfect transmission obtained already with five unit cells agree very well with the spin–orbit split minibands

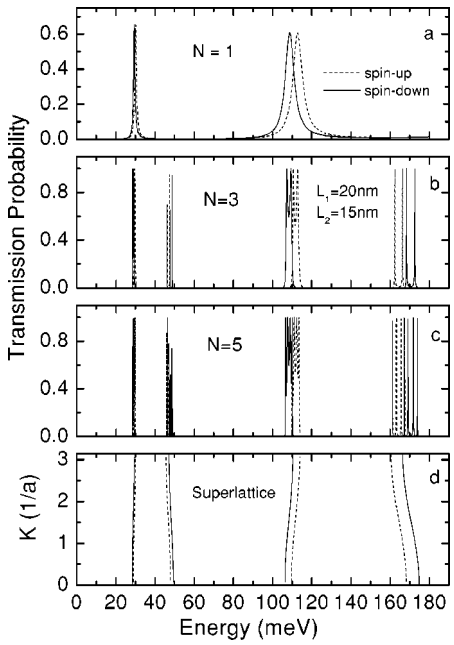

FIG. 3. Spin dependent transmission probability for electrons tunneling through the same structures in Fig. 2 exept for L_2 which was set here equal to 15 nm (panels a, b, and c), the asymmetric case. In the bottom panel (d), we show the spin–orbit split minibands obtained from the solution for the allowed electronic states and the corresponding asymmetric superlattice; note that the vertical axis in this case gives the Bloch wave vector.

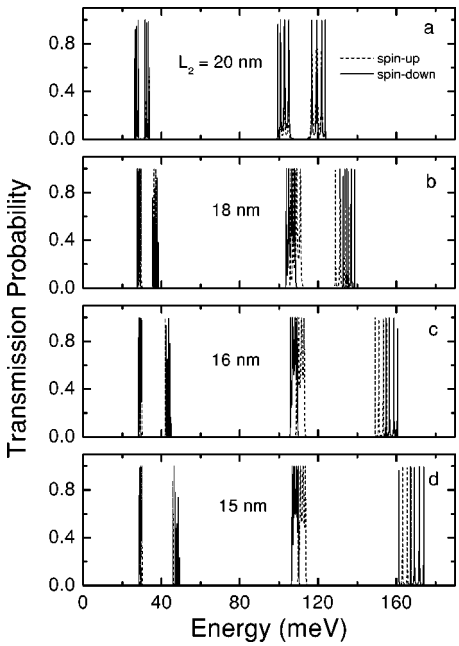

FIG. 4. Energy minibands with nonzero transmission for $N=5$ multibarrier structures with $L_1=20$ nm and varying L_2. The other parameters are as in Figs. 2 and 3. From panel a to panel d, L_2 is reduced, turning the structure more and more asymmetric, so that one can follow the mentioned symmetric–asymmetric crossover.

for the infinite superlattice. Next we describe the calculation of such minibands.

IV. SUPERLATTICE SPIN–ORBIT SPLIT MINIBANDS

If we set the x axis along $k_\parallel$, the total envelope function for the electron in the superlattice can be written as

$$\psi(r)=e^{ik_\parallel x}\phi(z), \tag{8}$$

and $\phi(z)$, as the solution of an effective one-dimensional Schrödinger equation with a periodic potential, will satisfy Bloch's theorem, i.e., $\phi(z+a)=e^{iKa}\phi(z)$, where K is the Bloch wave vector. As usual, solutions are obtained only within well defined energy minibands, which will in this case depend on both spin and $k_\parallel$, i.e., will be of the type $E_{k_\parallel,\pm}(K)$.

Probably, the simplest way to calculate such miniband structure is to write $\phi(z)$ as a linear combination of the linearly independent solutions for the transmissions through the unit cell from both, left and right, sides,[15] i.e., $\phi(z)=A\,\phi_l(z)+B\,\phi_r(z)$, where

$$\phi_l(z)=\begin{cases} e^{ik_z z}+r^l_\pm e^{-ik_z z}, & \text{on the left} \\ t^l_\pm e^{ik_z z}, & \text{on the right} \end{cases} \tag{9}$$

is the solution for incidence from the left and

$$\phi_r(z)=\begin{cases} t^r_\pm e^{-ik_z z}, & \text{on the left} \\ e^{-ik_z z}+r^r_\pm e^{ik_z z}, & \text{on the right} \end{cases} \tag{10}$$

for incidence from the right. Now, by applying Bloch's theorem, it is easy to obtain the following equation:

$$t^l_\pm e^{-iKa}+t^r_\pm e^{iKa}=(t^l_\pm t^r_\pm - r^l_\pm r^r_\pm)e^{ik_z a}+e^{-ik_z a}, \tag{11}$$

which, for every K (within 0 and π/a) and each spin, presents solutions only for a discrete set of energies. In the symmetric limit, when the transmission and reflection coefficients, t and r, are independent of both spin and side of incidence, we recover the usual, spin independent, equation for the superlattice minibands.[15] Solutions of the above equation for the asymmetric superlattice with $L_1=20$ nm and $L_2=15$ nm are shown in the bottom of Fig. 3, where we see the mentioned good agreement with the multibarrier transfer matrix calculation.

In Fig. 5 we show the results for the spin–orbit split minibands of asymmetric superlattices with different pairs of barrier materials. We note that the better spin resolved minibands occur for structures with GaAsSb and InP barriers. This is due to both, the large GaAsSb spin–orbit splitting Δ_{GaAsSb} and the bigger $|\Delta_{\mathrm{GaAsSb}}-\Delta_{\mathrm{InP}}|$ difference as compared to the other combinations. Figure 5 also shows that it is not difficult to obtain non overlapping opposite spin minibands. Such spin dependent miniband structure of perfect asymmetric superlattices leads to electron miniband transport that is very sensitive to electron spin. We see that, compared to the double-barrier case, the multibarrier or superlattice structure present narrower bands (or resonances) with higher transmission probability, which enhances the effect of spin-polarization by rosonant tunneling.

The perfect spin filtering, in the ideal case, corresponds to polarization of the transmitted beam being 1 (100%) for transmission within the spin up miniband and -1 within the

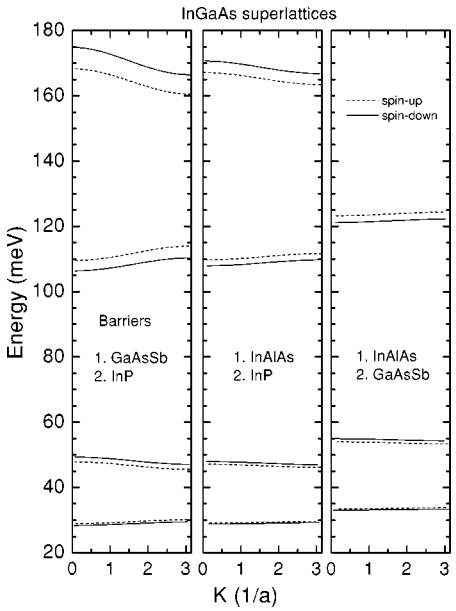

FIG. 5. Spin–orbit split minibands for asymmetric superlattices with different combinations of barrier materials, as calculated from the solution of Eq. (11). (Structure parameters are the same as in Fig. 3).

spin down miniband, except in the overlap or gap region, in between, where the polarization or the transmission, repectively, will be zero. The inevitable uncertainty in the angle of incidence (and/or electron energy) will however lead to the formation of miniband tails and to a decrease in the polarization. The effect due for instance to a given degree of uncertainty around the angle of incidence will depend on the angle, on the statistical distribution and on the energy one is looking at; and needs to be studied. We have estimated the effect of such angle uncertainty using a Gaussian distribution and have found that, for example, in the third miniband ($E \sim 110$ meV) of the situation in Fig. 3, a standard deviation of $\pi/100$ (corresponding to near 10% of uncertainty) leads to reasonable broadening of the minibands, which remain however well separated, and to a polarization which, as a function of energy, goes now smoothly from $+$ to -1. Polarizations close to the maximum are still obtained, with smaller transmission probabilities (~ 0.5) though, but with a larger energy separation between $+$ and -1. We have check also that the polarization becomes very small in the region of non zero transmission only with uncertainties as large as 25%.

V. CONCLUSIONS

In summary, we have considered the vertical quantum transport of polarized electrons along multibarrier and superlattice semiconductor structures. The superlattice miniband structure was discussed in accord to its symmetry under specular reflections along the growth direction. The formation of spin–orbit split minibands in the case of asymmetric superlattices, with asymmetric double-barrier unit cells, was demonstrated. Specific calculations were done for different InGaAs politype both multibarrier and superlattice structures. It was shown that the transfer matrix calculation reproduces well the superlattice spin resolved miniband structure with already three unit cells. The symmetric–asymmetric crossover as well as the miniband formation from the double barrier spin split resonances were also investigated.

The use of multibarrier structures, instead of a single asymmetric double barrier, enhances the effect of spin polarization by resonant tunneling. As shown here, it causes the narrowing the spin-split resonances and increases the transmission probability. The difficulty in the use of the effect, which is the oblique incidence, remains the same. However, continuum advances in nanolithografy and other technics for nanostructure design, allow us to believe that it may help the fabrication of powerful spin filters or other spintronic device in the near future. To conclude, we have discussed the formation of spin–orbit split minibands of electronic states in asymmetric III–V semiconductor superlattices, as a contribution to the physics of spin-dependent electronic properties of semiconductor nanostructures and to the development of the spintronics. Effects and corrections due for instance to the applied bias, electron–electron or electron–phonon interaction can be included within the present framework, but are outside the scope of this work.

ACKNOWLEDGMENTS

This work was partially supported by CNPq, CAPES, and FAPESP. We acknowledge helpful discussions with Professor G. C. La Rocca.

[1] See, for example, M. Johnson, Science **260**, 320 (1993); G. Prinz, Phys. Today **48**, 58 (1995); *Spin Eletronics*, edited by M. Ziese and M. J. Thornton (Springer, Berlin, 2001); Michael L. Roukes, Nature (London) **411**, 747 (2001).

[2] C.-M. Hu and T. Matsuyama, Phys. Rev. Lett. **87**, 066803 (2001); Th. Schäpers, J. Nitta, H. B. Heersche, and H. Takayanagi, Phys. Rev. B **64**, 125314 (2001); G. Schmidt, D. Ferrand, L. W. Molenkamp, A. T. Filip, and B. J. van Wees, *ibid.* **62**, R4790 (2000); H. B. Heersche, Th. Schäpers, J. Nitta, and H. Takayanagi, *ibid.* **64**, 161307 (2001).

[3] F. Mireles and G. Kirczenow, Phys. Rev. B **64**, 024426 (2001); L. W. Molenkamp, G. Schimidt, and G. E. W. Bauer, *ibid.* **64**, 121202 (2001).

[4] S. Datta and B. Das, Appl. Phys. Lett. **56**, 665 (1990).

[5] Yu A. Bychkov and E. I. Rashba, J. Phys. C **17**, 6039 (1984).

[6] The asymmetry mentioned here, and meant in the rest of the paper, is actually asymmetry under specular reflection around any point along the growth direction.

[7] See, for instance, E. A. de Andrada e Silva, Phys. Rev. B **46**, 1921 (1992); E. A. de Andrada e Silva, G. C. La Rocca, and F. Bassani, *ibid.* **50**, 8523 (1994); B. Jusserand, D. Richards, G. Allan, C. Priester, and B. Etienne, *ibid.* **51**, R4707 (1995); C.-M. Hu, J.

Nitta, T. Akazaki, H. Takayanagi, J. Osaka, P. Pfeffer, and W. Zawadzki, *ibid.* **60**, 7736 (1999); T. Matsuyama, R. Kursten, C. MeiBner, and U. Merkt, *ibid.* **61**, 15 588 (2000); D. Grundler, Phys. Rev. Lett. **84**, 6074 (2000).

[8] E. A. de Andrada e Silva and G. C. La Rocca, Phys. Rev. B **59**, R15 583 (1999).

[9] A. Voskoboynikov, S. Shin Liu, and C. P. Lee, Phys. Rev. B **59**, 12 514 (1999).

[10] See, for instance, *Properties of Lattice-Matched and Strained Indium–Gallium–Arsenide*, edited by P. Bhattacharya (INSPEC, London, 1993); Sadao Adachi, *Physical Properties of III–V Semiconductor Compounds* (Wiley, New York, 1992).

[11] J. Hu, X. G. Xu, J. A. H. Stotz, S. P. Watkins, A. E. Curzon, M. L. W. Thewalt, N. Matine, and C. R. Bolognesi, Appl. Phys. Lett. **73**, 2799 (1998).

[12] Superlattices with only one barrier material are sequences of symmetric quantum wells and present spin degenerate minibands even if asymmetric.

[13] For a recent example, see, J.H. Dickerson, E. E. Mendez, A. A. Allerman, S. Manotas, F. Agullo-Rueda, and C. Pecharroman, Phys. Rev. B **64**, 155302 (2001).

[14] E. A. de Andrada e Silva, G. C. La Rocca, and F. Bassani, Phys. Rev. B **55**, 16 293 (1997).

[15] N. W. Ashcroft and N. D. Mermin *Solid State Physics* (Saunders College Publishing, Orlando, 1976), Problem 1 of Chap. 8.